Refining Areal Quantification of Inland Waters and Assessing the Impact on Regional Carbon Budgets

James K. Mineau[1]

[1]Univerversity of Wisconsin – Madison; Madison, WI, USA; 0000-0002-2289-2252

Corresponding Author: James K. Mineau, 7156618620, jameskmineau@gmail.com

Keywords: inland waters, carbon, efflux, budget, lake, classification

Abstract:

Inland waters occur at a range of spatial scales and can drastically change over time. Globally, the size distribution of water bodies is skewed heavily towards smaller bodies. Due to previous mapping techniques, a significant number of these smaller bodies (< 0.1 sq. km) are not represented in global inland water databases. Generally, inland waters are considered net carbon sources to the atmosphere and relative to their size, smaller water bodies release more carbon into the atmosphere than larger bodies. Climate models rarely incorporate carbon cycling from inland waters. As remote sensing technologies become more accessible, the opportunity to remap and reevaluate carbon sources from inland waters presents itself. More accurate constraints on outgassing by inland waters would result in a further constrained global carbon budget.

Using 1 meter resolution hyperspectral imagery that was retrieved over a 10 km × 10 km region in northern Wisconsin in the summer of 2019, a high-resolution surface water map was created. Over this same sample period, an array of eddy covariance flux towers was positioned across different landscape types including permanent and seasonal lakes, as well as within wetlands. The combination of this dense network of flux towers and outgassing values from literature allows for average summer fluxes to be extrapolated across the region defined in the surface water map. Through the comparison of estimates using conventional inland water databases and this high-resolution surface water map, this study finds that carbon models underestimate the contribution of surface water to the total regional carbon budget.

Introduction

In the past few decades, inland waters have been identified as significant contributors to the global carbon budget (Cole et al. 2007; Raymond et al. 2013; Drake et al. 2018; Harmon 2020). This has only recently been the case, however, as the influence of inland water carbon cycling was limited to, initially, closed systems, followed by a period of treating inland waters as recipients of upstream influences. Today, inland waters are regarded as a considerable component of the global carbon budget (Tranvik et al. 2018). However, global climate models (GCMs) lag in their incorporation of inland waters into carbon cycling (Muster et al. 2013). Still regarded as a passive pipe within GCMs, inland waters are misrepresented, and this undercounting contributes to the large uncertainty present for the global terrestrial carbon sink (Cole et al. 2007). Minimizing the land sink uncertainty is essential to the greater goal of predicting future global greenhouse gas concentrations (Huntzinger et al. 2017). Therefore, additional effort should be made to incorporate our recent understanding on inland carbon cycling into GCMs.

Gas transfer theory – The interface between the water surface and atmospheric boundary layer serves to exchange gas concentrations to reach equilibrium within the boundary region (MacIntyre et al. 1995). Slightly soluble gases, such as carbon dioxide (CO_2) and methane (CH_4), have their exchange across the air-water interface inhibited by the aqueous boundary layer. Turbulence in the boundary region dominates the ability of slightly soluble gases (Crusius and Wanninkhof 2003). Gas exchange of CO_2 (F_c) can be estimated using the gas transfer velocity (k) and the gradient between the aqueous CO_2 concentration (C_w) and the atmospheric boundary layer concentration (C_a) modeled by the expression

$$F_c = k(C_w - \alpha C_a)$$

where α is the Ostwald solubility coefficient (MacIntyre et al. 1995). C_w is rarely measured in field campaigns and is difficult to estimate from limnological variables such as alkalinity (Kifner et al. 2018). Additionally, the gas transfer velocity requires either direct measurements of F_c, C_w, and C_a, or must be estimated via wind speed. However, for wind speeds less than about 3 m s^{-1}, which is characteristic of small lakes, the dependence of *k* on windspeed largely breaks down (Cole et al. 2010).

Due to this weakness of estimating gas transfer velocities and measuring CO_2 concentrations, the eddy covariance method has seen recent, limited use in measuring fluxes across the inland air-water interface (Anderson et al. 1999; Vesala et al. 2012). The eddy covariance method provides a direct, automated sampling regime that involves a relatively more complicated setup compensated by a reduction in investigator effort throughout a field campaign. This is unlike the floating chamber method or sampling of atmospheric and aqueous gas concentrations which require subsequent site visits by the investigator. The eddy covariance method makes use of the turbulent eddies that transport energy, water, and gases across space and time. The carbon dioxide vertical flux (F_c) can be calculated by the mean covariance between the deviations of vertical wind (w') and CO_2 mixing ratio (C') from the mean vertical wind ($\overline{w}$) and the mean CO_2 mixing ratio ($\bar{C}$), respectively, as the expression

$$F_c = \overline{w'C'}$$

where $w' = w - \overline{w}$ and $C' = C - \bar{C}$ (Anderson et al. 1999). While eddy covariance theory is relatively simply, the actual implementation and interpretation is not always as straight forward. Eddy covariance struggles at low speeds which can be a problem for sheltered, small ponds and lakes (Kenny et al. 2017). Additionally, eddy covariance theory is based on a homogeneous footprint, which is impossible for eddy covariance towers placed on a lake shore and unlikely for those floating near the terrestrial boundary (Reed et al. 2018; Morin et al. 2018). These complications require further consideration and care should be taken while interpreting results from lake situated eddy covariance towers.

Size dependence – Recently gaseous efflux from lakes and ponds have been determined to be partially a function of size (Downing 2010; Holgerson and Raymond 2016). Smaller water bodies generally are more supersaturated with respect to CO_2 than larger bodies. This is primarily due to the higher perimeter – area ratio for smaller bodies as well as smaller bodies generally being shallower (Holgerson and Raymond 2016). A higher perimeter – area ratio results in increased terrestrial carbon inputs in the form of decaying material through litterfall and surface runoff. Given the smaller water volume, carbon inputs to small bodies cause greater saturation than in larger bodies. Additionally, oxygen concentrations are generally lower in smaller ponds (Crisman et al. 1998; Downing 2010). The negative relationship between dissolved oxygen and pond CO_2 concentrations implies elevated CO_2 concentrations in smaller bodies (Holgerson 2015). As a result, small ponds and water bodies, despite only constituting 8.6% of lake area globally, contribute 15.1% of CO_2 emissions and 40.6% of diffusive CH_4 emissions (Holgerson and Raymond 2016).

Furthermore, the dominant force driving turbulence at the air-water boundary region varies by lake size between convection and wind shear (Read et al. 2012). Convection is of increasing importance for smaller lakes, while wind shear is generally a stronger influence for larger lakes, likely due to deeper boundary regions. This complicates estimates of k, which have historically been parametrized through wind speeds (Cole et al. 2010), as this results in a temporal dependence of k on wind. Convection lags wind shear, therefore, gas transfer estimates for small bodies, which are more dependent on convection for turbulence, will be based on the incorrect temporal signature of wind shear, rather than convection (Read et al. 2012).

Current estimates – Our understanding of both the spatial distribution of inland surface water, as well as the magnitude of which these bodies emit carbon to the atmosphere has rapidly increased in the past few decades (Tranvik et al. 2018). Currently, the highest resolution global inland water database available is the GLObal WAter BOdies database (GLOWABO), remotely sensed at 14.25 m spatial resolution (Verpoorter et al. 2014). GLOWABO consists of approximately 117 million lakes totaling 5×10^6 km^2 corresponding to 3.7% of Earth's nonglaciated land area. All lakes with a surface area of 0.002 km^2 are included; Caspian Sea not included. This dataset is not yet public. However, using the published distributions from GLOWABO, carbon emissions from lakes have been upscaled using a traditional extrapolation and a size-productivity weighted approach (DelSontro et al. 2018). The extrapolation approach following (Downing et al. 2006) yielded global carbon emissions from lakes and impoundments amounting to 4 C-CO_2eq yr^{-1}, while the size-productivity method resulted in 2.3 C-CO_2eq yr^{-1} (95% confidence interval). This size-productivity method is of similar magnitude to approximately 20% of global fossil fuel CO_2 emissions (DelSontro et al. 2018). Given the rapidly evolving knowledge base, it is not unreasonable to suggest that more progress is to be made both in regard to the global distribution of inland water and to the global carbon flux from these bodies.

Methods

CHEESEHEAD19 – The Chequamegon Heterogeneous Ecosystem Study Enabled by a High-density Extensive Array of Detectors 2019 (CHEESEHEAD19, cheesehead19.org) field campaign, a National Science Foundation project, serves as the parent project for this study

(Butterworth et al. 2021). During the growing season period (late June – late September) of northern Wisconsin, United States, CHEESEHEAD19 operated across a 10 km × 10 km domain in the Chequamegon-Nicolet National Forest (Figure 1).

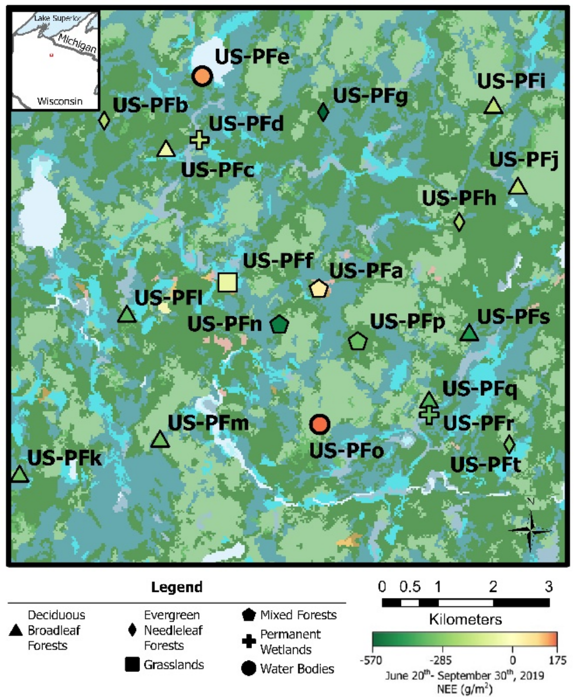

Figure 1. Map of CHEESEHEAD19 flux towers. Shape indicates land cover type. Color symbolizes net ecosystem exchange (NEE) over the study period (06/20-09/30/2019). Background is Wiscland2 data.

The primary objectives of CHEESEHEAD19 were to study the atmospheric boundary layer response to fluxes from a heterogeneous surface, investigate the energy balance closure problem, and identify issues in scaling surface fluxes. Using one of the world's highest density networks of eddy covariance flux towers throughout the observation period, combined with different profilers, daily radiosonde launches, and aerial imagery during three intensive observation periods, CHEESEHEAD19 provided data to tackle several scaling problems, including the scaling of inland water carbon fluxes from the local to, potentially, global scale (Butterworth et al. 2021).

Carbon fluxes – Flux towers positioned across the different land cover types are separated into five categories: Non-Water, Open, River, Vernal, and Wetland. An Open classification refers to larger, open bodies of water, while the Vernal classification are small, often temporary bodies. Fluxes are measured at half-hourly intervals. Mean CO_2 fluxes are then calculated for the period June 20th – September 30th, 2019, for each site (Table 1), before being averaged for each class (Figure 2). As no CHEESEHEAD19 flux towers were positioned over a river ecosystem, a mean yearly CO_2 flux for rivers is taken from (Crawford et al. 2014), who measured CO_2 fluxes using the floating chamber method over four rivers approximately 50 km from the CHEESEHEAD19 domain during 2012.

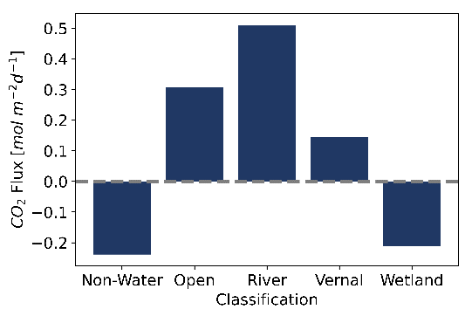

Figure 2. Mean summertime (6/20-9/30) CO2 fluxes. River flux is over an annual period (Crawford et al., 2014). All other values calculated from representative CHEESEHEAD19 flux towers.

*Hyperspectral imagery –H*yperspectral imagery was captured over the CHEESEHEAD19 domain from a Cessna 210 at 1400 m AGL across four days (June 26, July 11, August 4, August 30). This study exclusively uses the August 30th, 2019, imagery. With a spectral range spanning 400 – 2500 nm, the HySpex imager (VNIR-1800 and SWIR-384; HySpex, Skedsmokorset, Norway) provides 1-meter spatial resolution of the domain. The HySpex has a spectral resolution of 3.26 nm in the Visible and Near-Infrared (400-1000 nm) and 5.45 nm in the Shortwave Infrared (1000-2500 nm). For the August 30th acquisition, 25 flightlines were mosaiced to create a single image over the domain. Flightlines were georeferenced and bidirectional reflectance distribution function (BRDF) corrected.

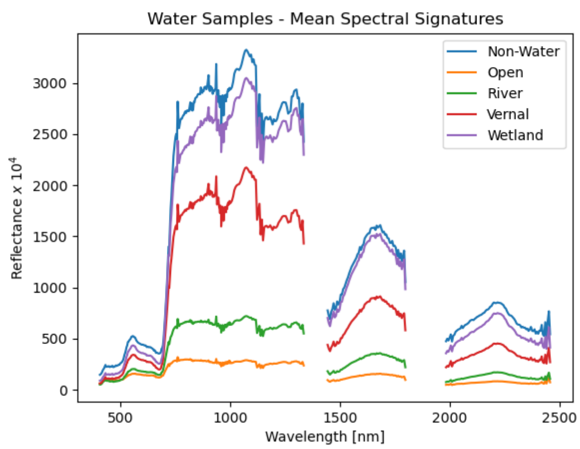

Figure 3. Hyperspectral signatures for ground truths.

HDWI – The Hyperspectral Difference Water Index (HDWI) was created using the hyperspectral mosaic (Xie et al. 2014). The HDWI takes advantage of the ‘red-edge’ difference between visible and near-infrared region to separate water from other surface types (Figure 3) and is calculated as follows

$$HDWI = \left[\int_{650\text{ nm}}^{700\ nm} R(\lambda)d\lambda - \int_{700\text{ nm}}^{850\ nm} R(\lambda)d\lambda\right] / \left[\int_{650\text{ nm}}^{700\ nm} R(\lambda)d\lambda + \int_{700\text{ nm}}^{850\ nm} R(\lambda)d\lambda\right]$$

Higher HDWI values indicate the surface is more likely to be inundated. Using ground truths collected during and following the field campaign, HDWI thresholds are iteratively tested to determine the threshold with the smallest summed errors of omission and commission. Road buffers are masked out as roads have a similar spectral signature. All pixels above this threshold value are categorized as Open, while all pixels below the threshold are considered Non-Water.

Results

Water distributions – Lake distributions and resulting CO_2 fluxes are compared to those used in prominent climate models. One of the most widely used land components of a climate model is the Community Land Model (CLM). The most recent version, CLM 5.0, utilizes the lake distribution Global Lakes and Wetlands Database (GLWD) to determine lake hydrography (Lehner and Döll 2004; Lawrence et al. 2019). Additionally, inundated surfaces are mathematically modeled as fractions of grid cells. CLM 5.0 includes methane surface fluxes as the ratio between CO_2 and CH_4. The HydroLAKES database is used as the lake hydrography for the Global Lake area, Climate, and Population dataset (Messager et al. 2016; Meyer et al. 2020). Finally, the National Hydrography Dataset – High Resolution, which provides the hydrography for the ~500,000 lakes greater than 1 hectare in the LAGOS-US (Spanish for lakes) LOCUS program (U.S. Geological Survey 2021; Cheruvelil et al. 2021). These three inland water datasets serve as a basis to compare the HDWI distribution findings from this study (Figure 4).

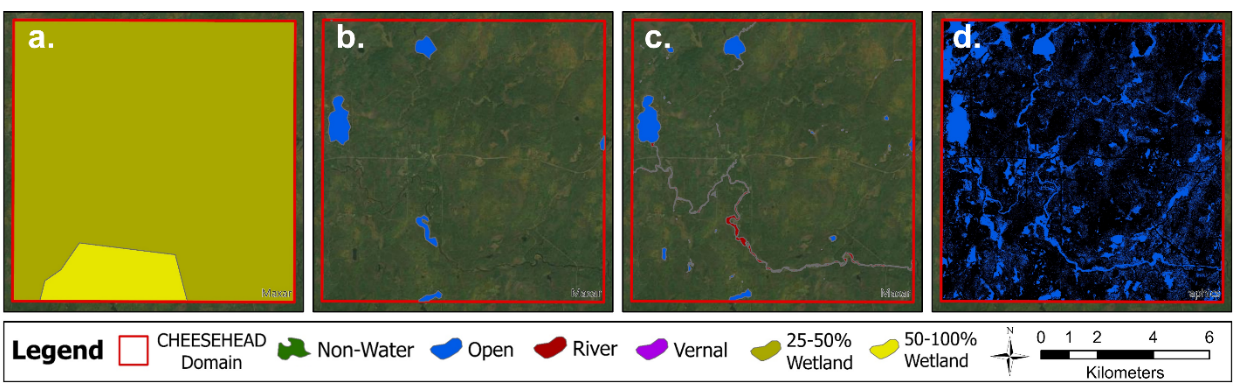

Figure 4. Inland waterbody distribution for the CHEESHEAD19 domain. ***a.*** *Global Lakes and Wetlands Database;* ***b.*** *HydroLAKES database;* ***c.*** *NHDPlus-HR;* ***d.*** *HDWI from CHEESEHEAD19 hyperspectral imagery, thresholded at -0.93*

The GLWD (Figure 4a) conceptualizes the CHEESEHEAD19 domain as 8.4% dense wetland (50-100% Wetland) and 92.6% as sporadic wetland (25-50% Wetland). Contrasting wetland interpretation, the HydroLAKES dataset (Figure 4b) contains six lakes totaling 1.79 km^2 within the CHEESEHEAD19 domain. The NHDPlus-HR (Figure 4c), which builds off HydroLAKES, includes the same bodies as HydroLAKES, but also incorporates the 10 m 3DEP digital elevation model and the WBD hydrologic-unit boundaries (U.S. Geological Survey 2021). For the CHEESEHEAD19 domain, NHDPlus-HR hosts 54 lakes/ponds covering 1.83 km^2 as well as two creeks and a river covering 0.88 km^2. Finally, the HWDI image (Figure 4d) produced from CHEESEHEAD19 hyperspectral imagery, with a threshold of -0.93, identifies 21.91 km^2 as being covered by surface water. The three hydrographies used in different models range in their representation of the CHEESEHEAD19 domain from idealizing the entire area as some fraction of wetland to identifying ~2% of the domain as covered by lakes and river, while this study finds that water covers approximately ~22% of the domain (Figure 5b). Additionally, the number of smaller lake bodies is significantly more from this work (Figure 5c).

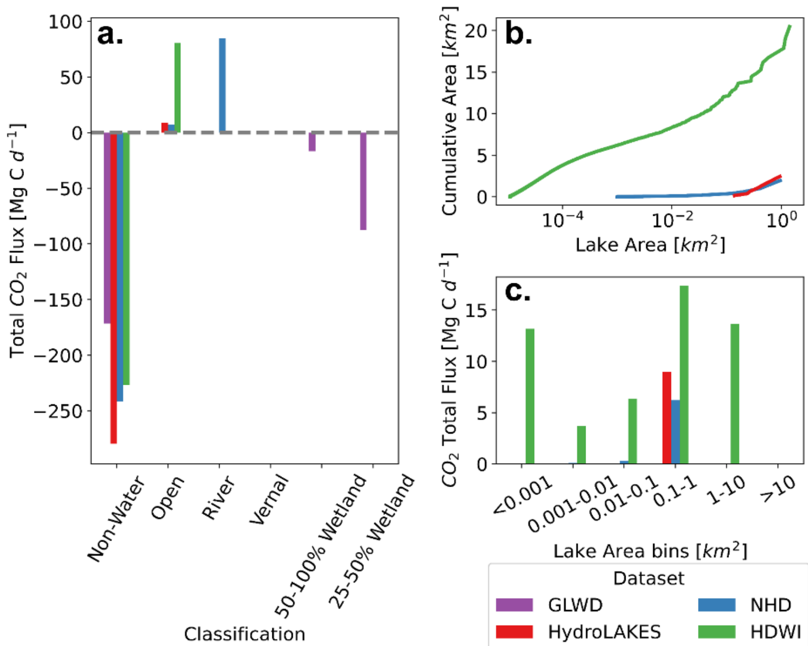

*Figure 5. **a.** Mean summertime fluxes extrapolated across CHEESEHEAD domain for each classification category and dataset. **b.** Cumulative lake area for each dataset with increasing lake area size. **c.** Extrapolated fluxes for lake area bins. When lake Area < 0.1 km^2 the Vernal flux is used; when lake Area ≥ 0.1 km^2 Open flux is used.*

Regional CO_2 fluxes – Representative CO_2 fluxes extrapolated to each dataset's hydrography, where areas that haven't been classified as water are treated as Non-Water, reveal large discrepancies, especially when comparing this work to others (Figure 5a). The GLWD represents the CHEESEHEAD19 domain as CO_2 sinks at all locations. The HydroLAKES and NHD exhibit small positive fluxes from Open water landcover, however, the inclusion of rivers into the NHD dataset results in a strong positive flux. Our thresholded HDWI water distribution indicates a large positive flux from Open water sources. No Vernal fluxes are represented in any dataset within the domain. Summing land cover classes across each dataset creates a simplified vertical CO_2 budget (Figure 6). Total regional CO_2 uptake for the NHD and HDWI datasets are approximately 120 Mg C less per day when compared to the GLWD and HydroLAKES datasets. This can primarily be attributed to the inclusion of rivers and small water bodies in the former datasets.

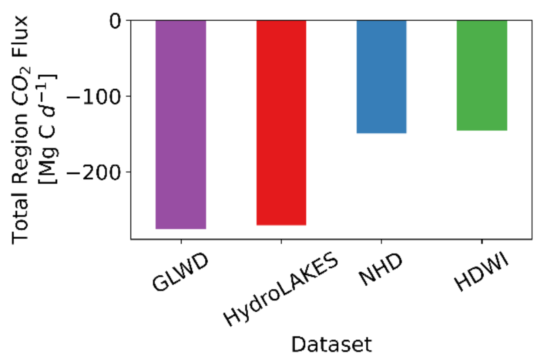

Figure 6. Total CO2 flux summed over classification categories for each dataset.

Discussion

Model comparison - Lake carbon dynamics are poorly represented within climate and lake models and budgets. Higher resolution data results in more positive CO_2 fluxes for the CHEESEHEAD19 domain. Much of the additional surface water area identified from the HDWI image is associated with bodies smaller than 0.1 km^2 (Figure 5c). Additionally, rivers are significant contributors of CO_2 to the atmosphere. Given their turbulent nature, rivers and streams have much higher gas transfer velocities. Acting as both transporters and emitters of carbon, river carbon dynamics require further investigation regarding climate modeling. However, it is important to remember that CHEESEHEAD19 lacked an eddy covariance tower with a river-dominated footprint and annual fluxes were used instead of growing season. As representing lake and surface water distributions appears to be the greatest difficulty for incorporating inland water carbon cycling into models, further effort and resources should be expended to create a global high resolution surface water map. As a result, lake rich regions such as the Northern Highlands Lake District of Wisconsin, adjacent to CHEESEHEAD19, have the potential to experience drastic changes in our understanding of their carbon budgets.

Implications for human populations – Humanity's continuing contribution to climate change has direct impacts on inland water carbon dynamics. As precipitation events become more extreme, both in terms of heavier rains and droughts, lakes and surface waters will receive increased surface runoff and will expose carbon rich sediments, respectively, likely increasing carbon emissions to the atmosphere (Tranvik et al. 2009; Marcé et al. 2019). Likewise, the rapid temperature changes occurring at high latitudes is resulting in significant glacial retreat and permafrost melt, exposing thermokarst lakes which are hotspots of carbon emissions, especially methane (Sepulveda-Jauregui et al. 2015). One of the most direct implications for human populations is the increasing trend in global eutrophication. Eutrophication has the potential to cause an additional 1 Pg CO_2eq yr^{-1} to be emitted to the atmosphere, which is approximately equal to 13% of global fossil fuel consumption (DelSontro et al. 2018). This is especially concerning as small agricultural ponds, which are supersaturated with carbon, cover about 77,000 km^2 globally and are more likely to experience eutrophication (Downing 2010). Additionally, eutrophication results in oxygen depletion, dead zones, and in some cases, fish kills, further complicating human - surface water interactions (Peterson et al. 2003). Finally, as water stresses escalate in regions of the world, damming of flowing waters has been shown to dramatically increase carbon emissions (Tranvik et al. 2009).

Conclusion

As stated by Downing et al. (2010), “little things mean a lot,” and this study has continued to prove that small inland waterbodies are significant components of regional, and likely global carbon cycling. Because climate change has significant impacts on inland water carbon dynamics, additional effort should be taken to embody these processes within climate models. Representing surface water distributions at a high resolution appears to be the main source of difficulty in properly incorporating these carbon fluxes to the atmosphere. Verpoorter et al.’s (2014) 14.25 m spatial resolution map likely has promise but has not been publicly released. Analysis of 1 m resolution imagery over a surface water dense region in northern Wisconsin indicates inland water hydrography datasets used for modeling oversimplify and under sample the amount of surface water.

Acknowledgements

The author extends an enormous amount of gratitude to Ankur Desai for his time as mentor and advisor. Prof. Desai’s guidance and outlook have had a positive, life-changing impact on the author. The work and mentorship of Brian Butterworth does not go unappreciated. B. Butterworth was an indispensable resource throughout the CHEESEHEAD19 field campaign as well as processing eddy covariance fluxes. Ting Zheng’s expertise with hyperspectral processing provided the basis for this analysis and could not have been done without her. The author would also like to thank Jim Mineau, U.S. Forest Service hydrologist, for his assistance in collecting ground truth data and Jerry Petruzalek, U.S. Forest Service GIS specialist, who provided local GIS data and expertise. Finally, the author acknowledges the time and effort provided by the entire CHEESEHEAD19 team and those of the UW-Madison Ecometeorology lab. This study was funded by NSF Award 1822420. CHEESEHEAD19 occurred on the traditional Ojibwe territory.

References

Anderson, D. E., R. G. Striegl, D. I. Stannard, C. M. Michmerhuizen, T. A. McConnaughey, and J. W. LaBaugh. 1999. Estimating lake-atmosphere CO2 exchange. Limnol. Oceanogr. **44**: 988–1001. doi:10.4319/LO.1999.44.4.0988

Butterworth, B. J., A. R. Desai, P. A. Townsend, and others. 2021. Connecting Land–Atmosphere Interactions to Surface Heterogeneity in CHEESEHEAD19. Bull. Am. Meteorol. Soc. **102**: E421–E445. doi:10.1175/BAMS-D-19-0346.1

Cheruvelil, K. S., P. A. Soranno, I. M. McCullough, K. E. Webster, L. K. Rodriguez, and N. J. Smith. 2021. LAGOS-US LOCUS v1.0: Data module of location, identifiers, and physical characteristics of lakes and their watersheds in the conterminous U.S. Limnol. Oceanogr. Lett. **6**: 270–292. doi:10.1002/LOL2.10203

Cole, J. J., D. L. Bade, D. Bastviken, M. L. Pace, and M. C. Van de Bogert. 2010. Multiple approaches to estimating air-water gas exchange in small lakes. Limnol. Oceanogr. Methods **8**: 285–293. doi:10.4319/lom.2010.8.285

Cole, J. J., Y. T. Prairie, N. F. Caraco, and others. 2007. Plumbing the Global Carbon Cycle: Integrating Inland Waters into the Terrestrial Carbon Budget. Ecosystems **10**: 172–185. doi:10.1007/s10021-006-9013-8

Crawford, J. T., N. R. Lottig, E. H. Stanley, J. F. Walker, P. C. Hanson, J. C. Finlay, and R. G. Striegl. 2014. CO2 and CH4 emissions from streams in a lake-rich landscape: Patterns, controls, and regional significance. Global Biogeochem. Cycles **28**: 197–210. doi:10.1002/2013GB004661

Crisman, T. L., L. J. Chapman, and C. A. Chapman. 1998. Predictors of Seasonal Oxygen Levels in Small Florida Lakes: The Importance of Color. Hydrobiol. 1998 3681 **368**: 149–155. doi:10.1023/A:1003289813849

Crusius, J., and R. Wanninkhof. 2003. Gas transfer velocities measured at low wind speed over a lake. Limnol. Oceanogr. **48**: 1010–1017. doi:10.4319/lo.2003.48.3.1010

DelSontro, T., J. J. Beaulieu, and J. A. Downing. 2018. Greenhouse gas emissions from lakes and impoundments: Upscaling in the face of global change. Limnol. Oceanogr. Lett. **3**: 64–75. doi:10.1002/lol2.10073

Downing, J. A. 2010. Emerging global role of small lakes and ponds: little things mean a lot. Limnetica **29**: 9–24. doi:10.23818/limn.29.02

Downing, J. A., Y. T. Prairie, J. J. Cole, and others. 2006. The global abundance and size distribution of lakes, ponds, and impoundments. Limnol. Oceanogr. **51**: 2388–2397. doi:10.4319/lo.2006.51.5.2388

Drake, T. W., P. A. Raymond, and R. G. M. M. Spencer. 2018. Terrestrial carbon inputs to inland waters: A current synthesis of estimates and uncertainty. Limnol. Oceanogr. Lett. **3**: 132–142. doi:10.1002/LOL2.10055

Harmon, T. C. 2020. Carbon gas flux to and from inland waters: support for a global observation network. Limnology **21**: 429–442. doi:10.1007/s10201-020-00623-1

Holgerson, M. A. 2015. Drivers of carbon dioxide and methane supersaturation in small, temporary ponds. Biogeochemistry **124**: 305–318.

Holgerson, M. A., and P. A. Raymond. 2016. Large contribution to inland water CO2 and CH4 emissions from very small ponds. Nat. Geosci. **9**: 222–226. doi:10.1038/ngeo2654

Huntzinger, D. N., A. M. Michalak, C. Schwalm, and others. 2017. Uncertainty in the response of terrestrial carbon sink to environmental drivers undermines carbon-climate feedback predictions. Sci. Reports 2017 71 **7**: 1–8. doi:10.1038/s41598-017-03818-2

Kenny, W. T., G. Bohrer, T. H. Morin, C. S. Vogel, A. M. Matheny, and A. R. Desai. 2017. A Numerical Case Study of the Implications of Secondary Circulations to the Interpretation of Eddy-Covariance Measurements Over Small Lakes. Boundary-Layer Meteorol. **165**: 311–332. doi:10.1007/S10546-017-0268-8/FIGURES/9

Kifner, L. H., A. J. K. Calhoun, S. A. Norton, K. E. Hoffmann, and A. Amirbahman. 2018. Methane and carbon dioxide dynamics within four vernal pools in Maine, USA. Biogeochemistry **139**: 275–291. doi:10.1007/S10533-018-0467-5/TABLES/7

Lawrence, D. M., R. A. Fisher, C. D. Koven, and others. 2019. The Community Land Model Version 5: Description of New Features, Benchmarking, and Impact of Forcing Uncertainty. J. Adv. Model. Earth Syst. **11**: 4245–4287. doi:10.1029/2018MS001583

Lehner, B., and P. Döll. 2004. Development and validation of a global database of lakes, reservoirs and wetlands. J. Hydrol. **296**: 1–22. doi:10.1016/J.JHYDROL.2004.03.028

MacIntyre, S., R. Wanninkhof, and J. P. Chanton. 1995. Trace Gas Exchange Across the Air-

Water Interface in Freshwater and Coastal Marine Environments, p. 52–97. *In* Biogenic Trace Gases: Measuring Emissions from Soil and Water.

Marcé, R., B. Obrador, L. Gómez-Gener, N. Catalán, M. Koschorreck, M. I. Arce, G. Singer, and D. von Schiller. 2019. Emissions from dry inland waters are a blind spot in the global carbon cycle. Earth-Science Rev. **188**: 240–248. doi:10.1016/J.EARSCIREV.2018.11.012

Messager, M. L., B. Lehner, G. Grill, I. Nedeva, and O. Schmitt. 2016. Estimating the volume and age of water stored in global lakes using a geo-statistical approach. Nat. Commun. **7**: 13603. doi:10.1038/ncomms13603

Meyer, M. F., M. R. Brousil, A. N. Cramer, B. P. Lanouette, J. C. Padowski, and S. E. Hampton. 2020. The Global Lake Area, Climate, and Population Dataset: A New Tool for Addressing Critical Limnological Questions. Limnol. Oceanogr. Bull. **29**: 110–116. doi:10.1002/lob.10406

Morin, T. H., A. C. Rey-Sánchez, C. S. Vogel, A. M. Matheny, W. T. Kenny, and G. Bohrer. 2018. Carbon dioxide emissions from an oligotrophic temperate lake: An eddy covariance approach. Ecol. Eng. **114**: 25–33. doi:10.1016/J.ECOLENG.2017.05.005

Muster, S., B. Heim, A. Abnizova, and J. Boike. 2013. Water Body Distributions Across Scales: A Remote Sensing Based Comparison of Three Arctic Tundra Wetlands. Remote Sens. **5**: 1498–1523. doi:10.3390/rs5041498

Peterson, G. D., T. D. Beard Jr., B. E. Beisner, E. M. Bennett, S. R. Carpenter, G. Cumming, C. L. Dent, and T. D. Havlicek. 2003. Assessing Future Ecosystem Services: a Case Study of the Northern Highlands Lake District, Wisconsin. Conserv. Ecol. **7**: art1. doi:10.5751/ES-00557-070301

Raymond, P. A., J. Hartmann, R. Lauerwald, and others. 2013. Global carbon dioxide emissions from inland waters. Nature **503**: 355–359. doi:10.1038/nature12760

Read, J. S., D. P. Hamilton, A. R. Desai, and others. 2012. Lake-size dependency of wind shear and convection as controls on gas exchange. Geophys. Res. Lett. **39**: 1–5. doi:10.1029/2012GL051886

Reed, D. E., H. A. Dugan, A. L. Flannery, and A. R. Desai. 2018. Carbon sink and source dynamics of a eutrophic deep lake using multiple flux observations over multiple years. Limnol. Oceanogr. Lett. **3**: 285–292. doi:10.1002/lol2.10075

Sepulveda-Jauregui, A., K. M. Walter Anthony, K. Martinez-Cruz, S. Greene, and F. Thalasso. 2015. Methane and carbon dioxide emissions from 40 lakes along a north-south latitudinal transect in Alaska. Biogeosciences **12**: 3197–3223. doi:10.5194/BG-12-3197-2015

Tranvik, L. J., J. J. Cole, and Y. T. Prairie. 2018. The study of carbon in inland waters—from isolated ecosystems to players in the global carbon cycle. Limnol. Oceanogr. Lett. **3**: 41–48. doi:10.1002/LOL2.10068

Tranvik, L. J., J. A. Downing, J. B. Cotner, and others. 2009. Lakes and reservoirs as regulators of carbon cycling and climate. Limnol. Oceanogr. **54**: 2298–2314. doi:10.4319/lo.2009.54.6_part_2.2298

U.S. Geological Survey. 2021. National Hydrography Dataset (ver. USGS NHDPlus High Resolution (HR) Beta.

Verpoorter, C., T. Kutser, D. A. Seekell, and L. J. Tranvik. 2014. A global inventory of lakes based on high-resolution satellite imagery. Geophys. Res. Lett. **41**: 6396–6402.

doi:10.1002/2014GL060641

Vesala, T., W. Eugster, and A. Ojala. 2012. Eddy Covariance Measurements over Lakes, p. 365–376. *In* Eddy Covariance. Springer Netherlands.

Xie, H., X. Luo, X. Xu, X. Tong, Y. Jin, H. Pan, and B. Zhou. 2014. New hyperspectral difference water index for the extraction of urban water bodies by the use of airborne hyperspectral images. J. Appl. Remote Sens. **8**: 085098. doi:10.1117/1.JRS.8.085098

Supplementary Materials

Table 1. CHEESEHEAD19 flux towers and their input classification for calculating mean fluxes over the field campaign.

Ameriflux Site	**Landcover**	**Classification**	**Mean CO_2 Flux [mol m^{-2} d^{-1}]**
US-PFa	Mixed Forests	Not Included	
US-PFb	Evergreen Needleleaf Forest	Non-Water	-0.172
US-PFc	Deciduous Broadleaf Forest	Non-Water	-0.035
US-PFd	Permanent Wetland	Wetland	-0.142
US-PFe	Water Body	Open	0.307
US-PFf	Grassland	Non-Water	-0.051
US-PFg	Evergreen Needleleaf Forest	Non-Water	-0.465
US-PFh	Evergreen Needleleaf Forest	Non-Water	-0.182
US-PFi	Deciduous Broadleaf Forest	Non-Water	-0.138
US-PFj	Deciduous Broadleaf Forest	Non-Water	-0.154
US-PFk	Deciduous Broadleaf Forest	Non-Water	-0.268
US-PFl	Deciduous Broadleaf Forest	Non-Water	-0.284
US-PFm	Deciduous Broadleaf Forest	Non-Water	-0.254
US-PFn	Mixed Forests	Non-Water	-0.406

US-PFo	Water Body	Vernal	0.144
US-PFp	Mixed Forests	Non-Water	-0.261
US-PFq	Deciduous Broadleaf Forest	Non-Water	-0.298
US-PFr	Permanent Wetland	Wetland	-0.279
US-PFs	Deciduous Broadleaf Forest	Non-Water	-0.363
US-PFt	Evergreen Needleleaf Forest	Non-Water	-0.248